Bioelectrochemistry 109 (2016) 79–86

Contents lists available at ScienceDirect

Bioelectrochemistry

journal homepage: www.elsevier.com/locate/bioelechem

Influence of various sterilization procedures on TiO_2 nanotubes used for biomedical devices

Ita Junkar [a,*], Mukta Kulkarni [b], Barbara Drašler [c], Neža Rugelj [c], Anca Mazare [d], Ajda Flašker [b], Damjana Drobne [c], Petr Humpolíček [e], Matic Resnik [a], Patrik Schmuki [d], Miran Mozetič [a], Aleš Iglič [b]

[a] Jožef Stefan Institute, Jamova cesta 39, Ljubljana SI-1000, Slovenia
[b] Laboratory of Biophysics, Faculty of Electrical Engineering, University of Ljubljana, Tržaška 25, Ljubljana SI-1000, Slovenia
[c] Department of Biology, Biotechnical Faculty, University of Ljubljana, Večna pot 111, 1000 Ljubljana, Slovenia
[d] Department of Materials Science and Engineering, WW4-LKO, University of Erlangen Nuremberg, Martensstr. 7, 91058 Erlangen, Germany
[e] Centre of Polymer Systems, University Institute, Tomas Bata University in Zlin, Nad Ovcirnou 3685, 760 01 Zlin, Czech Republic

ARTICLE INFO

Article history:
Received 20 October 2015
Received in revised form 4 February 2016
Accepted 7 February 2016
Available online 10 February 2016

Keywords:
TiO_2 nanotubes
Sterilization
Surface
Cytocompatibility
Electrochemical anodization

ABSTRACT

Sterilization is the final surface treatment procedure of all implantable devices and is one of the key factors which have to be considered before implementation. Since different sterilization procedures for all implantable devices influence mechanical properties as well as biological response, the influence of different sterilization techniques on titanium nanotubes was studied. Commonly used sterilization techniques such as autoclaving, ultra-violet light sterilization, hydrogen peroxide plasma sterilization as well as the not so frequently used gaseous oxygen plasma sterilization were used. Three different nanotube diameters; 15 nm, 50 nm and 100 nm were employed to study the effects of various sterilization techniques. It was observed that autoclave sterilization resulted in destruction of nanotubular features on all three studied nanotube diameters, while UV-light and both kinds of plasma sterilization did not cause any significant morphological changes on the surfaces. Differences between the sterilization techniques employed influenced cytocompatibility, especially in the case of nanotubes with 100 nm diameter.

© 2016 Elsevier B.V. All rights reserved.

1. Introduction

Due to its superior mechanical properties Titanium (Ti) is widely used in medicine, especially as an orthopaedic, dental or even vascular implant. Ti implants have an essential role in medicine and biotechnology as they possess unique mechanical properties and have anticorrosive and biocompatible surface properties due to the formation of a protective titanium dioxide (TiO_2) layer [1,2]. It has been shown that the spontaneously formed oxide layer on Ti surface is not uniform and that it varies in thickness from 2–10 nm [3,4], which influences on biological response (*e.g.* cells or tissue). Recently many attempts were made to improve Ti surface properties, mainly by nanostructuring, which includes formation of TiO_2 nanotubule (NT) surface [5]. NTs have high potential, not only as biomaterials [6–8], but also as materials used for photocatalysis, photoelectrolysis, sensing and for solar cells [9–13]. The excellent and unique potential of NT surfaces in medicine and biotechnology is due to their high surface to volume ratio and the possibility that an NT can be fabricated in different diameters and lengths. This allows for the design of nanostructured surfaces for their specific application, because biological (*e.g.* cells or tissue) and physiological systems (*e.g.* blood coagulation or immune response) can respond differently to distinct topographic features. *In vitro* studies have already shown that surface features at the nanometre scale stimulate and control several molecular and cellular events on the tissue/implant interface, which can be observed by differences in cell morphology, orientation, cytoskeleton organization, proliferation and gene expression [14–18]. Moreover, several studies have revealed considerable impact of TiO_2 NT surfaces on osteoblast differentiation [19,20] as well as on proliferation and subsequent mineralization of the extracellular matrix [21], which makes such surfaces ideal for their use in orthopaedic applications as well as for dental implants. The estimated market size of orthopaedic implants in 2009 alone was estimated at $33 billion with prognosis of 7.1% year-to-year increase [22]. This clearly shows that there is an enormous demand for orthopaedic implants with superior properties. NT surfaces certainly have a high potential for use as orthopaedic implants due to their simple and inexpensive fabrication and also their appropriate biological response. They have been shown to increase bone growth/regeneration [23,24], are antibacterial [25–27] and reduce inflammation [28,29]. Many studies deal with the effects of Ti NTs on the biological response, however results are not overall consistent. It has been shown that enhanced functions of osteoblast cells are obtained on NTs between 15 and 70 nm in diameter [5,7,9,10,30]. Parke et al. reported that NTs with a diameter between 15 and 30 nm

* Corresponding author.
E-mail address: Ita.junkar@ijs.si (I. Junkar).

http://dx.doi.org/10.1016/j.bioelechem.2016.02.001
1567-5394/© 2016 Elsevier B.V. All rights reserved.

enhance the activity of osteoblast, while cell proliferation and migration on tube diameters larger than 70 nm was significantly reduced [31]. Moreover Oh et al. [21] reported that the cell seeding density and type of sterilization used (wet or dry autoclaving) significantly influence adhesion and proliferation of osteoblast cells on NT surfaces, especially for the case of 70 and 100 nm diameter. Prominent differences in osteoblast proliferation after 24 and 48 h of incubation on freshly prepared TiO_2 NT surfaces and TiO_2 NT surfaces following heat treatment were also observed. It was shown that osteoblast cell proliferation on heat treated NTs was improved, which was explained by the presence of the anatase phase in the TiO_2 NT after heat treatment, as well as by possible remaining fluorine (introduced during HF anodization) on freshly prepared NTs [32]. Because small changes in surface properties of the NTs significantly influence on the proliferation and migration of cells it is important to explore the effects of different treatment techniques on physical and chemical properties of NT surfaces. Sterilization presents the final surface treatment step of medical materials and may influence the NT surface morphology and their chemical composition. Therefore the sterilization of NT surfaces presents an important aspect which should be considered, while preparing NT surfaces for medical applications. Not only in terms of possible infections but also in terms of altered surface properties and its influence on cytocompatibility. As different sterilization techniques and their influence on NT morphology and surface chemistry are still not fully understood [27,32], it was our aim to study the effects of different sterilization techniques on the topological, physical and chemical properties of TiO_2 NT surfaces with different diameters. We were particularly interested in observing changes in surface morphology of NT and their influence on cytocompatibility *in vitro*.

For the purpose of our work, NT surfaces with different diameters were produced by electrochemical anodization and the influence of various sterilization techniques on specific surface morphology was studied. Changes in surface morphology after common sterilization techniques, such as autoclaving, ultra-violet (UV) light exposure and commercial hydrogen peroxide (H_2O_2) plasma, were assessed using scanning electron microscopy (SEM), atomic force microscopy (AFM) and water contact angle measurements (WCA). Moreover, a non-commercial sterilization technique by gaseous oxygen plasma was studied, as it represents an interesting approach for sterilization as well as for modification of the top surface layer of NTs, with a high potential to improve surface biocompatibility. Effects of sterilization techniques on cytocompatibility *in vitro* were studied using model human osteoblasts (HObs), by applying conventional colorimetric viability assay coupled with SEM imaging.

2. Materials and methods

2.1. Preparation of titanium dioxide nanotubes

Titanium dioxide (TiO_2) nanotubular (NT) surfaces were obtained by electrochemical anodization of Ti foils of 0.1 mm thickness, 99.6% purity. Prior to anodization, Ti foils were degreased by successive ultrasonication steps in acetone, ethanol and deionized (DI) water respectively for 5 min each and dried in a nitrogen stream. Ethylene glycol based electrolytes containing specific concentrations of water and hydrofluoric acid were used to obtain desired dimensions of NT, as was shown in our previous work [33,34]. All the anodization experiments were carried out at room temperature with platinum gauze as the counter electrode and Ti foil as anode, with a working electrode distance of 15 mm. As-formed, TiO_2 nanostructured surfaces were kept in ethanol for 2 h to remove all organic components from the electrolyte, washed with distilled water and dried in a nitrogen stream. The three different diameters of NT were prepared; 15 nm (NT15), 50 nm (NT50) and 100 nm (NT100) which were further analysed for their morphological features, wettability and *in vitro* cytocompatibility.

2.2. Sterilization of TiO_2 NT

2.2.1. Sterilization with autoclave

NT surfaces were transferred into glass petri dishes, and autoclaved at for 15 min (high pressure and saturated steam at 105–135 °C; Table-top autoclave A-21CA; Kambič laboratorijska oprema, Semič, Slovenia). For transferring and handling the NT samples, sterile tweezers (70% ethanol (EtOH) and fire-exposed) were used.

2.2.2. Sterilization with ultra-violet (UV) light radiations

Sterile tweezers (70% EtOH and fire-exposed) were used to transfer the NT surfaces into a 12-well culture plate. Approximately 1 mL of 70% EtOH was added in the well plate to dip NT sample completely. After 10 min incubation, EtOH was removed and the sample was left open in a sterile laminar hood until EtOH evaporated completely. Then, the samples were exposed to UV light at 253.7 nm wavelength (at a distance of app. 40 cm from the UV-light source; PHILIPS TUV 36W G13, Philips, Nevada Industrial, USA) in a sterile laminar hood for 20 min. The intensity of UV-light, used for sterilization of the TiO_2 surfaces, was measured spectrophotometrically using a Flame UV–VIS spectrophotometer (Ocean optics, USA; device source: FLMS00202; light source: Osram Lumilux combi EL-N 36 W), in the interval between 240 and 850 nm, with the sensor placed at the same position as the irradiated samples. A standard output low pressure mercury lamp (Hg LP lamp; SEN Lights, Crystec Technology Trading GmbH, Germany) was used for sensor calibration from 180 to 600 nm and the classic rectangular method was applied for the integration. The results were expressed as μWatt/cm^2. The analysis of the UV–VIS spectrum (240 to 850 nm) showed the main peak at 254 nm and the rectangular integration analysis collective showed communal intensity of $1.35 \cdot 10^4$ W/cm^2.

2.2.3. Commercial hydrogen peroxide plasma

NT surfaces were packed in self-sealed sterilization packaging (Arrowpack, Ljubljana, Slovenia) and treated with hydrogen peroxide plasma (Sterrad S100, Johnson&Johnson Medical Ltd, NJ, USA) for 54 min (short cycle).

2.2.4. Oxygen plasma treatment

Treatment of NT surfaces was conducted by oxygen plasma in the plasma reactor. Detailed information about the plasma reactor is published in our previous paper [35]. Shortly the gaseous plasma was created with an inductively coupled RF generator, operating at a frequency of 13.56 MHz and an output power set at 200 W. Commercially available oxygen was leaked into the discharge chamber. The pressure was fixed at 75 Pa as at this pressure the highest degree of dissociation of oxygen molecules has been measured using a catalytic probe [36]. The samples were treated for 60 s and then packed in sterile containers. Scheme 1 is schematic representation of the RF plasma reactor.

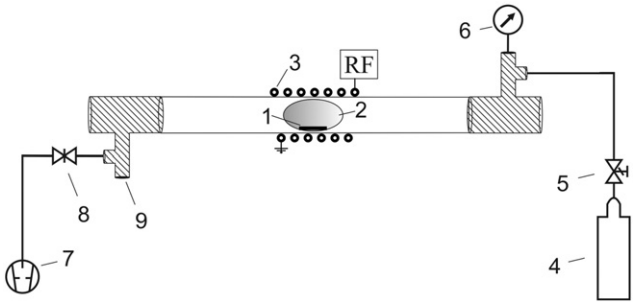

Scheme 1. Schematic representation of the radiofrequency (RF) plasma reactor used for treatment of NT and Ti foil. 1: sample, 2: plasma glow region, 3: RF coil, 4: working gas,5: inlet valve, 6: vacuum metre,7: vacuum pump, 8: outlet valve, 9: air inlet.

2.3. Water contact angle (WCA) measurements

The wettability of NT surfaces of different diameters as well as of plain Ti foil was studied by water contact angle (WCA) measurements. A droplet of demineralized water (3 μL volume) was put on the NTs surface and images of Ti and NT surfaces were captured before and after sterilization procedure. For each sample 10 measurements were performed in order to minimize the statistical error. The relative humidity was kept at 45% and the temperature at 25 °C. The contact angles were measured by an Advex Instruments See System E equipped with a CCD camera and a PC computer, which enabled us to make high resolution pictures [33]. The values of WCA were determined by the See System 6.3 software, which enables fitting of the water drop on the surface in order to allow a relatively precise determination of WCA. An estimated error for each WCA value was less than 3.0°.

2.4. Morphology analysis by scanning electron microscopy (SEM) and atomic force microscopy (AFM)

To observe changes in the morphological features of NTs, SEM (Jeol JSM-7600F, USA) analysis was employed. The analysis was done at accelerating voltage of 8 keV and the samples with cells were prior to SEM analysis sputtered with gold (5 nm coating). Changes in surface morphology of the 100 nm NT surfaces and Ti surfaces after different sterilization techniques were analysed by atomic force microscopy (AFM, Solver PRO, NT-MDT, Russia) in tapping mode in air. Samples were scanned with a standard Si cantilever with a force constant of 22 N/m and at a resonance frequency of 325 kHz (tip radius was 10 nm and the tip length was 95 μm). The average surface roughness (Ra) was measured from representative images of $1 \times 1\ \mu m^2$ area and at a scan rate set at 1.3 Hz.

2.5. Osteoblast cell culture cultivation and its exposure to NT surfaces

Since osteoblasts are a relevant *in vitro* model system to study the biological compatibility of materials intended for bone implants, we selected primary human osteoblast (HOb) line for assessment of cytocompatibility on sterilized NT surfaces with different diameters of NT. The HOb cell line was purchased from the European Collection of Cell Cultures (ECACC; Public Health England, Salisbury, UK) and cultured in growth medium for HOb cells (Cell applications, Inc. San Diego, CA 92121, USA) in a humidified atmosphere of 5% CO_2/95% air at 37 °C. Cells were routinely subcultured once a week or when they reached 65–70% confluence. Before harvesting with Trypsin-0.25% EDTA (Sigma-Aldrich, Steinheim, Germany) for approximately 10 min at 37 °C, cells were washed three times with Phosphate Buffered Saline without Ca^{2+} and Mg^{2+} (PBS; Sigma-Aldrich, Steinheim, Germany). Cells were then resuspended in the growth medium, centrifuged at 200*g* for 5 min, and plated at a seeding density of 1×10^4 cells per cm^2 of tissue culture 24-well plates (Sigma-Aldrich, TPP ®, Steinheim, Germany) containing the plain Ti or nanorough surfaces (NT 15, 50 or 100 nm), in 1 mL of growth medium. 24 h after seeding and subsequently every 48 h, the medium was removed (1 mL) and changed with a fresh aliquot. HOB cells were grown on surfaces sterilized by the different above-presented techniques. After 1 week of growth under controlled conditions (5% CO_2/95% air at 37 °C), the cells were further processed for either fixation for SEM, or for cell viability assays. The fixation procedure for SEM analysis is described below.

2.5.1. Fixation for scanning electron microscopy (SEM)

After a predefined time of incubation (1 week), the cell culture medium was removed, cells were washed with PBS and fixed for 2 h at room temperature using a modified Karnovsky fixative, composed of 2.5% glutaraldehyde (SPI Supplies, West Chester, PA, USA) and 0.4% paraformaldehyde (Merck KGaA, Darmstadt, Germany) in 1 M Na-phosphate buffer ($NaH_2PO_4\ 2{\cdot}H_2O$ and $Na_2HPO_4\ 2{\cdot}H_2O$; all the chemicals from Merck KGaA, Darmstadt, Germany). After 3 h, the fixative was removed and 1 M Na-phosphate buffer was added; the samples were left in the fridge over the night. Then the samples were washed in the buffer for 3×10 min and the post-fixation of samples was undertaken with 1% osmium tetroxide (OsO_4) (SPI Supplies, West Chester, PA, USA; 1×60 min), followed by washing in dH_2O 3×10 min, incubation in thiocarbohydrazide (TCH; Sigma-Aldrich, Steinheim, Germany) for 20 min, washing in dH_2O 3×10 min, incubation in OsO_4 1×20 min and washing in dH_2O 3×10 min. Samples were dehydrated with 30% ethanol (EtOH; Merck KGaA, Darmstadt, Germany) (10 min), 50% EtOH (10 min), 70% EtOH (10 min; left overnight at 4 °C), 80% EtOH (10 min), 90% EtOH (10 min) and absolute EtOH (10 min). Further dehydration steps were conducted with a mixture of Hexamethyldisiloxane (HMDS; SPI Supplies, West Chester, PA, USA) and absolute EtOH (1:1; v/v; 10 min), 3:1 (HMDS: absolute EtOH, v/v; 10 min) and absolute HMDS (10 min), which was left to evaporate for 24 h.

2.5.2. Cell viability assessment: MTT assay

The viability of HOb cells grown on the tested TiO_2 NT and Ti foil surfaces was assessed using a common assay based on the activity of NAD(P)H-dependent cellular oxidoreductase enzymes, capable of reducing the tetrazolium dye 3-(4,5-dimethylthiazol-2-yl)-2,5-diphenyltetrazolium bromide (MTT; ≥97.5%, Sigma-Aldrich, Steinheim, Germany) to insoluble formazan [37].

At the end of the pre-selected incubation period (1 week exposure), cells grown on TiO_2 NT and Ti foil surfaces were washed 3 times with PBS and were transferred into a clean 24-well plate and 0.3 mL of freshly prepared growth medium supplemented with 5 mg/mL of MTT (30 μL) was added to each well (final concentration 0.5 mg MTT/mL). After 3 h of incubation at 37 °C, the medium was removed, and formazan crystals were dissolved by addition of 250 μL of DMSO per well. For quantification, 250 μL of sample was transferred into 96-well plate and absorbance of formazan (A(570 nm) and the formazan background A(690 nm)) was measured (Cytation 3 Cell Imaging Multi-Mode Reader, BioTek® Instruments, Inc., Vermont, USA). The background absorbance values (A(690 nm)) were subtracted from the absorbance values A(570 nm). Surface area of the plain Ti foil or NT covered surfaces was estimated from photographs of the tested surfaces, using ImageJ v. 1.48. The subtracted absorbance values of cells grown on plasma-treated surfaces (plain Ti or NT 15, 50 or 100) were normalized to the absorbance values for cells grown on plain Ti foil.

3. Results and discussion

3.1. Wetting behaviour of TiO_2 nanotubes

Water contact angle (WCA) measurements were made in order to determine the wetting behaviour of fresh and sterilized NT and Ti foil surfaces. The pristine Ti foil had a WCA value about 77° and its value decreased to about 55° for autoclaved samples and to about 34° for UV-light sterilized samples, while the plasma treated Ti foil was practically superhydrophilic. All NT surfaces were hydrophilic, as observed in our previous work [33] these samples tend to age within about three weeks' time and slowly become hydrophobic. Therefore, all *in vitro* biological experiments were conducted on freshly prepared NT surfaces. The freshly prepared NT surfaces were sterilized and the superhydrophilic effects were observed in all cases. Thus different sterilization procedures did not influence wettability of NT.

3.2. Morphology of nanotubular layers after sterilization

The characterization of NT surfaces was performed by SEM and AFM in order to study the changes in morphology on TiO_2 NTs after the use of different sterilization techniques. TiO_2 NT surfaces with nanotube diameter of 15 nm, 50 nm and 100 nm [38] were studied. After sterilization with autoclaving, significant changes in surface morphology were

observed, namely, the nanotubular features of the NT surfaces were to a large extent destroyed (see Fig. 1, first column of autoclave sterilization). From all the three different NT diameters the least disrupted nanotubular surface features were observed on NT100 (showing some sintering of the structures and thickening of the tube walls). In the case of NT50 the nanotubes were destroyed but some porosity was still preserved, whereas the smaller diameter nanotubes (NT15) show sintering/collapse of all the NTs, meaning that practically all the NT features are lost. It should be emphasised that the destruction of the NTs was also observed in the z-direction, as the results from cross-section analysis (data not shown) confirm that the bottom of NT were destroyed. In some parts the bottom imprints were still observed, but the tubes were mashed together. After UV sterilization, a slight disruption of NT was observed, mainly their ordered structure was affected, see Fig. 1, second column of UV sterilization. An intact nanotubular surface structure was observed after oxygen plasma or commercial plasma sterilization, as shown for oxygen plasma treatment in Fig. 1, third column (data not shown for commercial plasma).

We suggest that the primary cause of NT destruction in an autoclave might be the combined effect of moisture and a high temperature, exceeding 92 °C (in the case of steam autoclave sterilization), which induces crystallization of the amorphous TiO_2 NTs and results in changed morphology [38,39]. Although it is known that anodized TiO_2 NTs are generally stable in their amorphous phase to temperatures of about 300 °C [40], this is not true if the NTs are exposed to vapour [38]. The mechanism proposed for water vapour or water crystallization as well as the modification in the NT morphology is discussed by Lamberti et al. [39] and Wang et al. [41]. In our case the temperature of autoclave sterilization was 121 °C and the surface was exposed to vapour. Briefly, the water vapour molecules interact with the amorphous TiO_2 nanotube walls and condensate as hot water that further acts as a catalyst favouring the rearrangement of TiO_6^{2-} octahedra [39,42]; in addition, a decrease in the contact angle is also reported due to the formation of surface defects that act as adsorption sites for –OH [39]. Thus, the observed changes in the NT surface morphology (see Fig. 1, first column) can be assigned to the combined effects of vapour and temperature exceeding 92 °C. Moreover, it should be emphasised that sterilization with an autoclave is done at higher temperatures, as compared with other sterilization techniques employed in this work, thus it is possible that fluoride ions from the NT surface evaporate due to high temperature [43]. Fluoride is found in low concentration on all the NT surfaces fabricated by anodization due to its presence in the electrolytes [33,34] and may as well cause some destruction of NTs.

By contrast, the NT surfaces treated by UV-light and plasma sterilization methods did not show any prominent changes in surface morphology. This is consistent with existing literature data reporting a cleaning effect of UV sterilization without surface alteration [27,42,44] that decreases the hydrocarbon contamination (that is, the UV treatment removes carbon contamination by either the induced photocatalytic activity of TiO_2 or their direct decomposition by UV) [44,45]. For plasma sterilization methods, the superficial removal of contaminants/material or so called etching is observed with slight increase in surface roughness as well as modification in surface activity (*e.g.* oxygen plasma leads to a higher affinity for molecule adsorption) [32] — for an overview see Reference [46]. The fact that in our study no significant changes in the NT morphology were observed is mainly governed by the lower temperature during the sterilization procedure and the absence of water molecules (vapour), which decreases the chances of fluoride evaporation and crystallization/modification of NTs. However, in the case of UV-light sterilization we have noticed small changes in NT morphology, as the top of the NTs appeared slightly etched and there was small debris mostly present at the rim of the tube top, as seen in Fig. 1 (second column), which was more evident in the case of NT50 and NT100).

Additional information about NT morphology alterations after different sterilizations were acquired by AFM. Only the images for the NT100 are shown (Fig. 2) as the AFM analysis on smaller diameter NTs did not provide enough information due to inability of the AFM tip to enter the hollow interiors of smaller diameter NTs (less than 50 nm). Disruption of NTs was clearly observed for the autoclaved samples (Fig. 2a, phase and height images), where in some cases nanotubes seem to be broken and closed at the top, which is in accordance with SEM results (Fig. 1, first column).

UV-light sterilization did not have much influence on surface morphology (Fig. 2b). Similar NT surface topography was observed for NT100 sterilized either with commercial H_2O_2 plasma (data not shown) or oxygen plasma (Fig. 2c). From phase images, after both UV-light

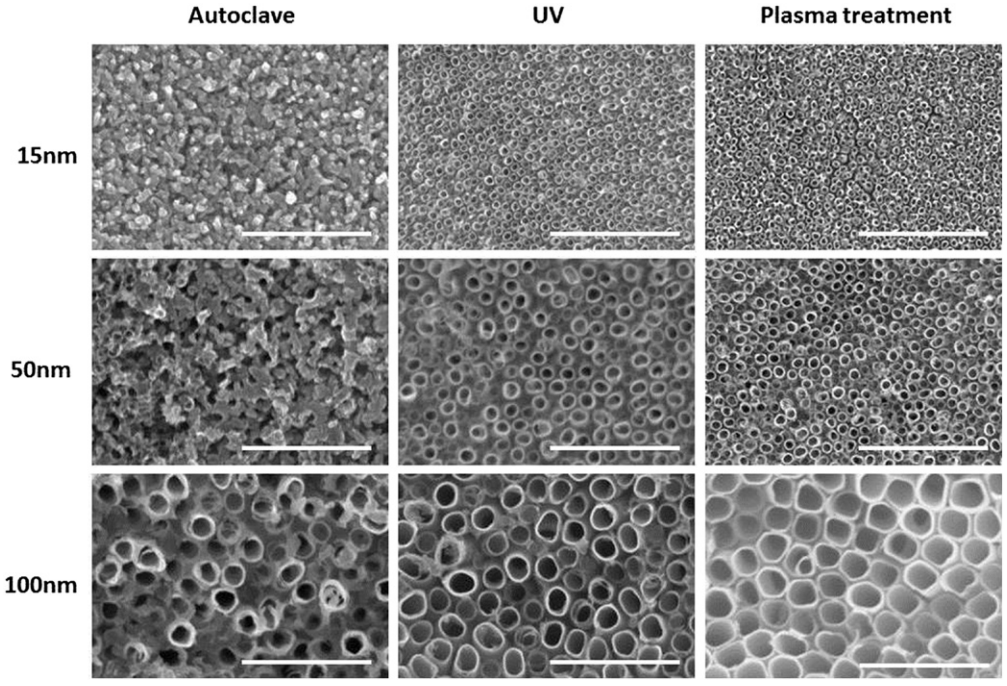

Fig. 1. SEM images of nanotubes with 15 nm (NT15), 50 nm (NT50) and 100 nm (NT100) in diameter after sterilization with autoclave (first column), UV-light (second column) and after oxygen plasma treatment (third column). Scale bar: 1 μm.

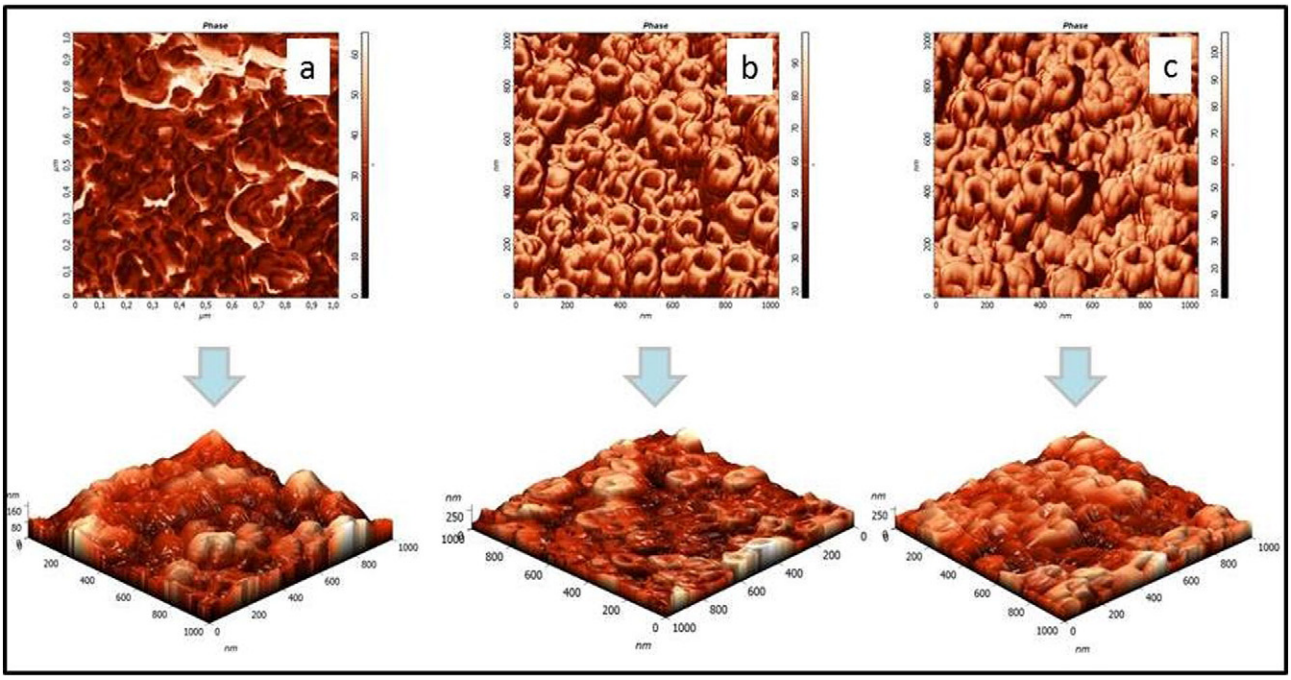

Fig. 2. AFM images of nanotubes with 100 nm in diameter sterilized with a) autoclave, b) UV-light and c) plasma treatment. In upper panel are the phase images and in lower panel the corresponding 3D images of the surface.

and plasma sterilization (Fig. 2b and c), a uniform nanotubular structure was clearly seen without any disruption of surface topography. In addition, AFM analysis of the pristine Ti foil was conducted in order to evaluate surface morphology and the results showed fairly flat topography with no special features on the surface (data not shown). The measured surface roughness (Ra) on $1 \times 1\ \mu m^2$ of plain Ti foil had Ra of about 11.8 ± 3 nm, while slightly higher roughness was detected on autoclaved NT100 surfaces (Ra of about 23 ± 2 nm). The highest roughness was measured on both UV-light sterilized and plasma treated NT100 surfaces with Ra 37.3 ± 3 and 35.7 ± 2 nm, respectively. Similar values were measured also for the untreated NT100. This information is valuable for further *in vitro* studies, as Ti surface morphology plays an important role in cytocompatibility.

3.3. In vitro cytocompatibility

Cytocompatibility is a complex of cell characteristics, such as the ability of cells to adhere on the surface and subsequently grow, proliferate and differentiate on it in a physiological manner. Besides this, appropriate gene expression and extracellular matrix formation are also important factors showing the realistic cytocompatibility of any material. However, the presented study mainly focused on the impact of various sterilization techniques on surface properties of TiO_2 NT, thus only the basic cell–surface interactions were detected. Specifically, the quantification of viable cells on the NT surfaces was detected using an MTT assay and cell morphology was determined by using SEM.

3.3.1. Cell morphology

It was observed that all autoclaved NT surfaces exhibited different morphology/behaviour of HOb cells regardless of the NT diameter when compared to the autoclaved plain Ti foil. Only a limited number of cells, mainly in a non-spread form, was observed on the autoclaved NT surfaces, while many fully spread cells were observed on the control material (autoclaved plain Ti foil) (Fig. 3a and b). The main reason for the observed low interaction of HOb cells with the autoclaved NT surfaces may be the disrupted top surface nanotubular features, which were observed by SEM and AFM (Figs. 1 and 2). The closed nanotubular topography with slightly higher roughness and higher wettability in comparison to the autoclaved plain Ti foil seem to affect cell physiology and subsequently cell morphology. Cells grown on oxygen plasma sterilized control surfaces (plain Ti foil) and on the NT15 surfaces are presented in Fig. 3c and d. In both cases, cells were attached predominantly in a widely spread form. A similar phenomenon was also observed for the oxygen plasma treated NT50 and NT100 surfaces (images not shown). It can be seen that filopodia of cells grown on the autoclaved plain Ti foil (Fig. 3a) are not elongated, which indicates a lower strength of interaction of cells with the surface [47]. In the case of plasma treated Ti foils filopodia appeared to be elongated (Fig. 3c). Similar behaviour was noticed for cells grown on oxygen plasma sterilized NT surfaces; cells seemed to interact closely with each other as well as with the surface, which is seen from their elongated form and long filopodia (Fig. 3d). It can be concluded from Fig. 3 that oxygen plasma treatment, even on plain Ti foil, improves the strength of interaction of HOb cells with the surface. This effect is quite interesting, especially if we compare the autoclaved Ti foil and plasma sterilized Ti foil. Improved interaction of HOb cells could be explained by the increased thickness and density of the oxygen layer on the surface of Ti foil, which is formed after exposure to highly reactive oxygen species in plasma, as well as due to superhydrophilicity of the Ti foil surface after such treatment. All plasma treated surfaces are superhydrophilic, while the autoclaved Ti foil has WCA of about 55°.

In order to better observe alterations in the morphology of filopodia of cells, grown on oxygen plasma treated surfaces, higher magnification images are presented in Fig. 4. From these images (Fig. 4) it can be seen that cells on plain oxygen plasma treated Ti foil and on the oxygen plasma treated NT15 and NT50 surfaces are in elongated form and have long filopodia, while less elongated cell morphology was observed on the NT100 surfaces treated by oxygen plasma (Fig. 4d). It seems that the large hollow interior of NT100 influences adhesion and proliferation of HOb cells, which could be mainly explained by difference in protein adsorption for different nanotopographic features [34].

A comparison of HOb attachment on oxygen plasma treated NT15, NT50 and NT100 surfaces is presented in Fig. 5. Some alterations in morphology of HOb cells were observed for cells grown on NT15 and NT50 surfaces, namely, cells appeared to be more spread, which presumably stimulates filopodia to connect with the nanorough 15 nm and 50 nm

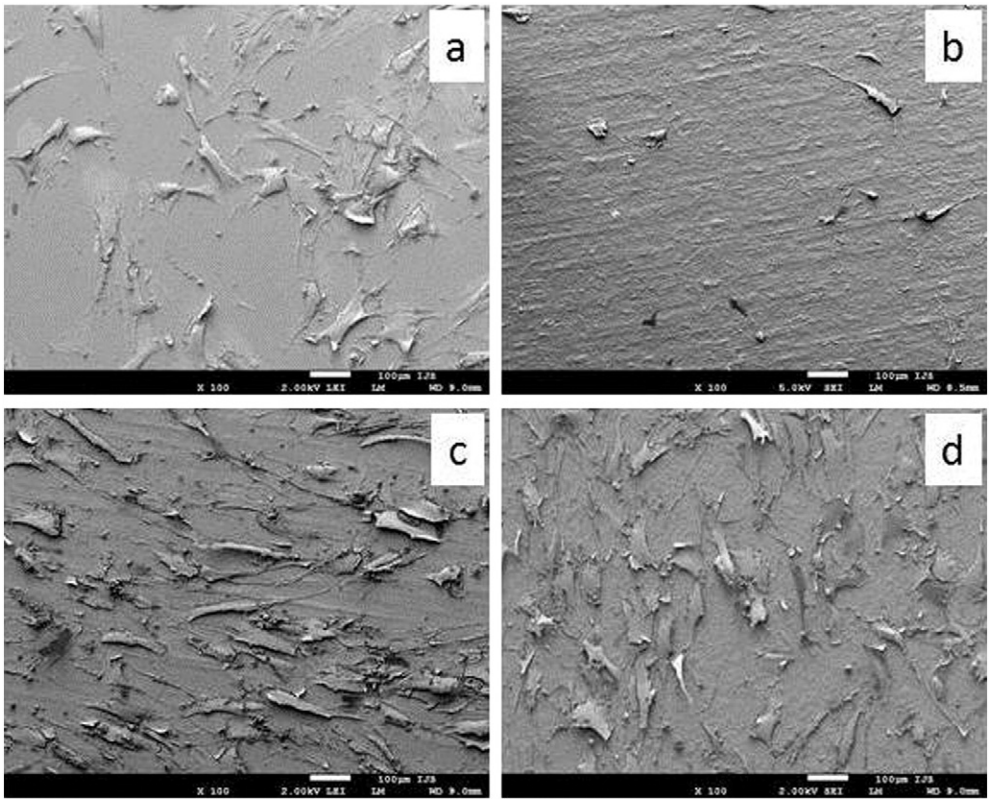

Fig. 3. SEM images of interaction of HOb cells with a) Ti foil, sterilized with autoclave, b) nanotubes with NT15 sterilized with autoclave, c) Ti foil, sterilized with plasma treatment and d) NT15 sterilized with plasma treatment.

surfaces. More extended filopodia are indeed observed for NT15 surfaces and NT50 surfaces, even at lower magnification, as cells developed prolonged shape of filopodia reaching far and interacting with nearby cells (Fig. 5c, upper panel). However this was not observed for the NT100 surfaces, as cells did not seem to interact so strongly and practically no extended filopodia were observed on these surfaces (Fig. 5c,

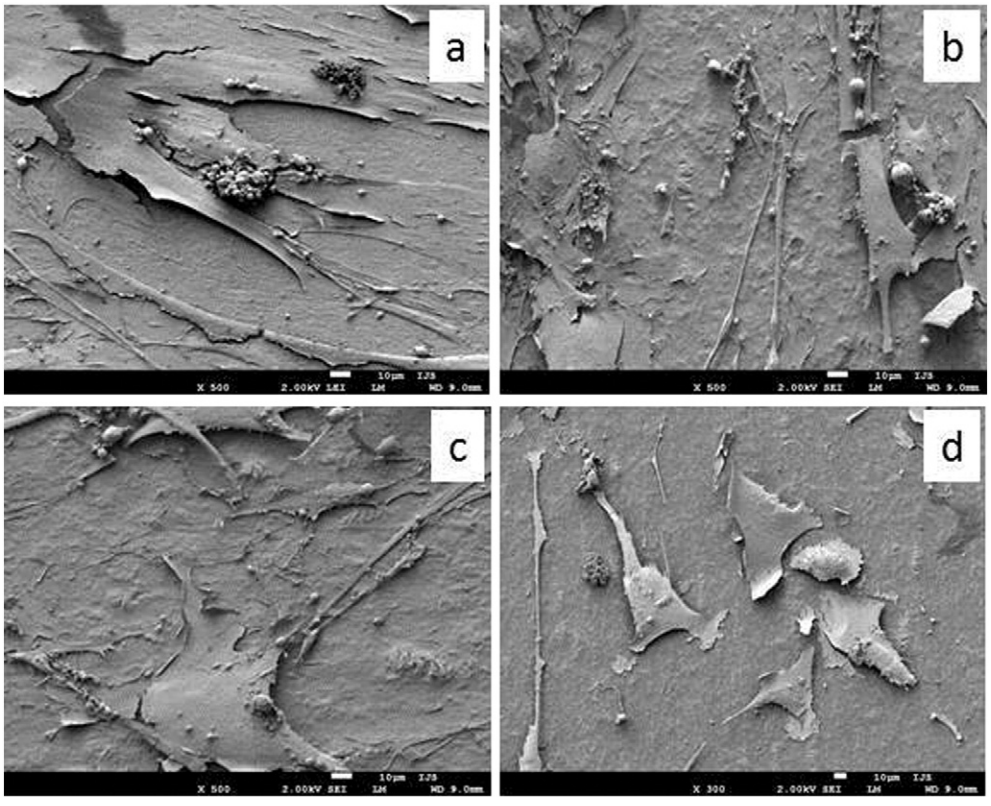

Fig. 4. High magnification SEM images of HOb cell interacting with a.) Ti foil, b.) NT15, c.) NT50 and d.) NT100.

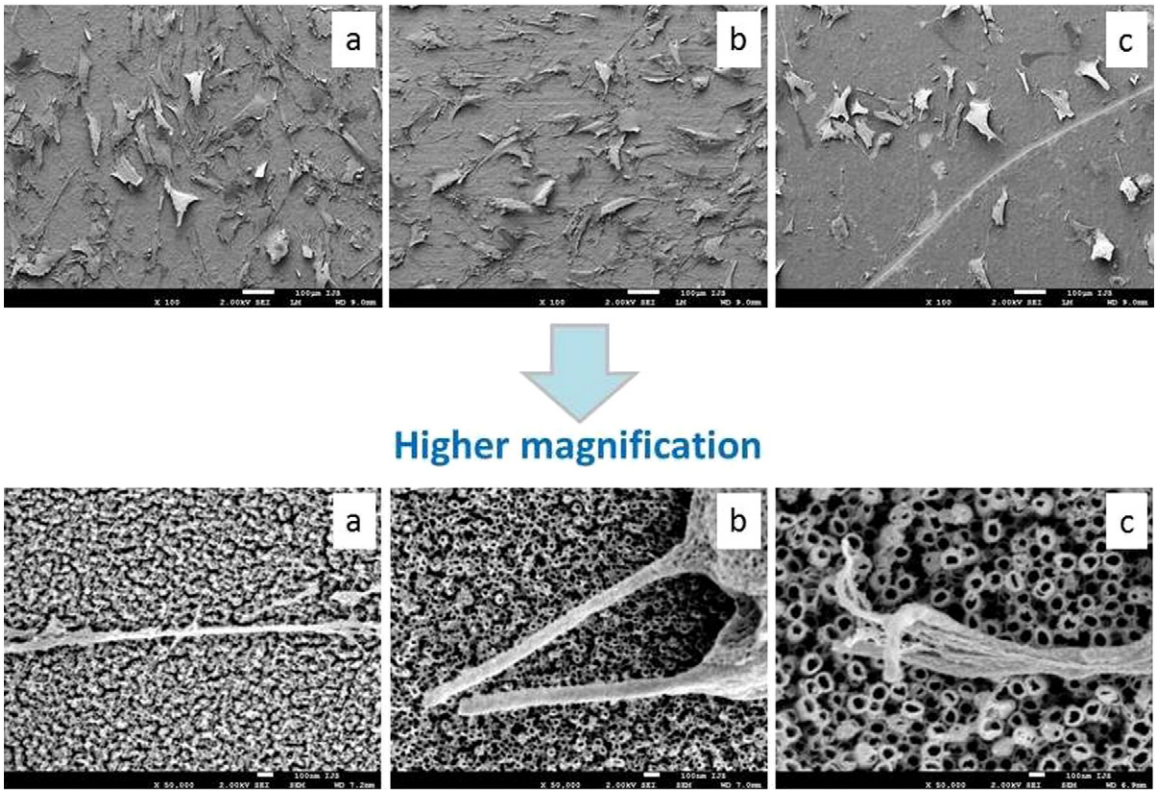

Fig. 5. SEM image of HOb cells interacting with plasma treated surface a.) NT15, b.) NT50 and c.) NT100.

upper panel). At higher magnification, interaction of filopodia with the NT surfaces are presented (Fig. 5, lower panel). From these images we can observe that filopodia of HOb cells are highly interacting with the surface of NT15 and NT50 surfaces, while lower interaction seems to take place on NT100 surfaces.

3.3.2. Cell viability

The number of viable cells was assessed by MTT assay after one week of cultivation on Ti foil and different NT surfaces. The lowest number of cells, grown on the plain Ti foil and NT100 surfaces sterilized with UV-light, in comparison to the other tested surfaces (NT15, NT50 with both UV-light and oxygen plasma sterilization and plain Ti foil and NT100 with oxygen plasma) was observed. Interestingly all the oxygen plasma treated surfaces exhibited improved viability of HOb cells at given experimental conditions *in vitro* (seeding density of 1×10^4 cells/cm^2; 1-week exposure; MTT assay) (Fig. 6). The latter observed phenomenon suggests that oxygen plasma treatment of Ti and NT surfaces was effective in enhancing cell viability of HOb cells. Cell viability was increased by a factor of 1.4 already on plasma sterilized plain Ti foil in comparison to the UV-sterilized Ti foil. Moreover, according to the MTT assay, the morphological features of the surface also influenced on cell viability. Namely, regardless of the sterilization procedure (UV or plasma treatment), a reduced viability of cells grown on NT100 was observed compared with plain Ti foil, NT15 or NT50 samples.

This above is in line with results obtained by other groups [16,31] as well as with our studies on HOb morphology obtained by SEM (Fig. 4). The results from the MTT assay clearly show that not only different surface nanotopography, but also the type of sterilization used, significantly influences cell–surface interactions. Although no morphological features were altered after UV-light or oxygen plasma treatment of NT, some differences in cytocompatibility *in vitro* were detected. Namely, a significantly higher number of viable cells were observed on oxygen plasma treated NT100 surfaces in comparison to UV-light sterilized NT100. Although both surfaces had a similar surface roughness and exhibited superhydrophilic character, the observed changes could be ascribed to altered chemical composition of the surface upon application of different sterilization techniques. It is already known that autoclave sterilization of titanium implants is associated with increased hydrocarbon contamination, while UV-light sterilization decreases hydrocarbon contamination which is associated with formation of abundant Ti–OH functional groups [43]. Whereas for the case of oxygen plasma treatment of titanium foil as well as of NTs, the surface is exposed to highly reactive oxygen species, which interact with the surface and decrease hydrocarbon contamination and form a denser oxide (TiO_2) layer on the surface (for the case of oxygen plasma treatment). It should be emphasised that Ti foil also exhibits a naturally formed TiO_2 layer on

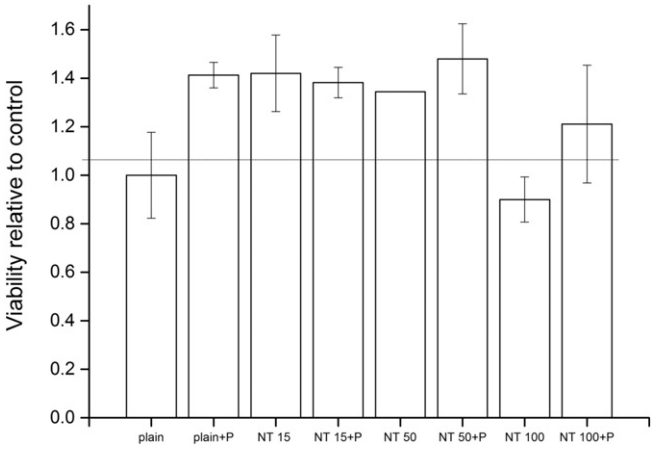

Fig. 6. Cell viability expressed by MTT assay, for cells grown on the UV-light or plasma (P) sterilized surfaces. Comparative values of cell viabilities of plasma treated samples were calculated with respect to the reference material (plan Ti-foil); marked as a horizontal line). Abbreviations: plain = plain Ti-foil, P = plasma treated surface, 15 = NT15 nm, 50 = NT50 nm, 100 = NT 100 nm. Number of analysed samples: 1 (NT 50), 2 (plain, NT 15, NT 100) or 3 (all the plasma treated surfaces) per tested group.

the surface, which is altered after exposure to oxygen plasma. Much of the changes in surface properties of the TiO_2 layer can be attributed to changes in surface chemistry and wettability, which strongly influence its overall bioactivity. Such treatment influences the top oxide layer which becomes denser, has lower hydrocarbon contamination and becomes more hydrophilic.

Therefore differences in cell viability between UV-light and oxygen plasma sterilization of NT100 could be ascribed to the formation of a thicker oxygen layer, which is already known to be correlated with improved biocompatibility of the surface. Moreover, according to the *in vitro* cytocompatibility results, a similar explanation can be given for the observed differences between the plain Ti foils treated by UV-light and oxygen plasma.

4. Conclusions

The results of the present study indicate that different sterilization techniques may have a significant influence on surface properties of TiO_2 NT surfaces and, consequently, also on their cytocompatibility *in vitro*. It was shown that steam autoclaving is not an appropriate sterilization technique for TiO_2 NT surfaces, as it results in distraction of NT features. UV-light, commercial H_2O_2 plasma sterilization and oxygen plasma treatment techniques did not influence on NT surface features. However, differences between these sterilization techniques were observed, as it was shown that the type of sterilization significantly influences on *in vitro* cytocompatibility of HOb cells with TiO_2 NT. Although it was shown that NT features play an important role in cell–material interactions, the influence of the final surface treatment procedure (sterilization) has to be considered. Therefore determining the appropriate sterilization technique for TiO_2 NT surfaces is one of the key factors which should be carefully selected before their application in cellular and tissue systems.

Acknowledgement

The authors would like to thank the Slovenian Research Agency (ARRS) grants J1-4109, J1-4136, J3-4108, P3-0314 and P2-0232 for its financial support.

This work was supported by the Ministry of Education, Youth and Sports of the Czech Republic Programme NPU I (LO1504).

The authors are grateful to Dr. Andrej Meglič (Biotechnical faculty, University of Ljubljana) and Dr. Rok Zaplotnik (Jožef Stefan Institute) for the measurements of UV-light intensity.

References

[1] B. Feng, et al., Characterization of surface oxide films on titanium and adhesion of osteoblast, Biomaterials 24 (25) (2003) 4663–4670.
[2] M. Kulkarni, et al., Titanium nanostructures for biomedical applications, Nanotechnology 26 (6) (2015) 062002.
[3] E.P. Lautenschlager, P. Monaghan, Titanium and titanium alloys as dental materials, Int. Dent. J. 43 (3) (1993) 245–253.
[4] L. Carlsson, et al., Osseointegration of titanium implants, Acta Orthop. 57 (4) (1986) 285–289.
[5] M. Kulkarni, et al., Biomaterial surface modification of titanium and titanium alloys for medical applications, Nanomedicine, Manchaster, UK Central Press 2014, pp. 111–136.
[6] M. Bigerelle, et al., Improvement in the morphology of Ti-based surfaces: a new process to increase in vitro human osteoblast response, Biomaterials 23 (7) (2002) 1563–1577.
[7] E. Gongadze, et al., Adhesion of osteoblasts to a nanorough titanium implant surface, Int. J. Nanomedicine 6 (2011) 1801.
[8] E. Gongadze, et al., Adhesion of osteoblasts to a vertically aligned TiO_2 nanotube surface, Mini-Rev. Med. Chem. 13 (2) (2013) 194–200.
[9] S. Liu, A. Chen, Coadsorption of horseradish peroxidase with thionine on TiO_2 nanotubes for biosensing, Langmuir 21 (18) (2005) 8409–8413.
[10] M. Paulose, et al., Anodic growth of highly ordered TiO_2 nanotube arrays to 134 μm in length, J. Phys. Chem. B 110 (33) (2006) 16179–16184.
[11] O.K. Varghese, C.A. Grimes, Metal oxide nanoarchitectures for environmental sensing, J. Nanosci. Nanotechnol. 3 (4) (2003) 277–293.
[12] K. Zhu, et al., Enhanced charge-collection efficiencies and light scattering in dye-sensitized solar cells using oriented TiO_2 nanotubes arrays, Nano Lett. 7 (1) (2007) 69–74.
[13] H.-H. Ou, S.-L. Lo, Review of titania nanotubes synthesized via the hydrothermal treatment: fabrication, modification, and application, Sep. Purif. Technol. 58 (1) (2007) 179–191.
[14] S. Oh, et al., Influence of sterilization methods on cell behavior and functionality of osteoblasts cultured on TiO_2 nanotubes, Mater. Sci. Eng. C 31 (5) (2011) 873–879.
[15] M. Dalby, et al., In vitro reaction of endothelial cells to polymer demixed nanotopography, Biomaterials 23 (14) (2002) 2945–2954.
[16] J. Park, et al., Narrow window in nanoscale dependent activation of endothelial cell growth and differentiation on TiO_2 nanotube surfaces, Nano Lett. 9 (9) (2009) 3157–3164.
[17] C. Mohan, et al., In vitro hemocompatibility and vascular endothelial cell functionality on titania nanostructures under static and dynamic conditions for improved coronary stenting applications, Acta Biomater. 9 (12) (2013) 9568–9577.
[18] A. De Mel, et al., Surface modification of biomaterials: a quest for blood compatibility, Int. J. Biomater. (2012) (2012: p).
[19] M. Rubert, et al., Effect of TiO_2 scaffolds coated with alginate hydrogel containing a proline-rich peptide on osteoblast growth and differentiation in vitro, J. Biomed. Mater. Res. A 101 (6) (2013) 1768–1777.
[20] A. Verket, et al., Enhanced osteoblast differentiation on scaffolds coated with TiO_2 compared to SiO_2 and CaP coatings, Biointerphases 7 (1) (2012) 36.
[21] S. Oh, et al., Significantly accelerated osteoblast cell growth on aligned TiO_2 nanotubes, J. Biomed. Mater. Res. A 78 (1) (2006) 97–103.
[22] L. Wood, The top 10 orthopedic device companies, Bus. Insights (2010) (Accessed August 2).
[23] S. Puckett, et al., Nano rough micron patterned titanium for directing osteoblast morphology and adhesion, Int. J. Nanomedicine 3 (2) (2008) 229.
[24] L.M. Bjursten, et al., Titanium dioxide nanotubes enhance bone bonding in vivo, J. Biomed. Mater. Res. A 92 (3) (2010) 1218–1224.
[25] B. Ercan, et al., Diameter of titanium nanotubes influences anti-bacterial efficacy, Nanotechnology 22 (29) (2011) 295102.
[26] S.D. Puckett, et al., The relationship between the nanostructure of titanium surfaces and bacterial attachment, Biomaterials 31 (4) (2010) 706–713.
[27] K.M. Kummer, et al., Effects of different sterilization techniques and varying anodized TiO_2 nanotube dimensions on bacteria growth, J. Biomed. Mater. Res. B Appl. Biomater. 101 (5) (2013) 677–688.
[28] P. Neacsu, et al., Reduced inflammatory activity of RAW 264.7 macrophages on titania nanotube modified Ti surface, Int. J. Biochem. Cell Biol. 55 (2014) 187–195.
[29] A. Rajyalakshmi, et al., Reduced adhesion of macrophages on anodized titanium with select nanotube surface features, Int. J. Nanomedicine 6 (2011) 1765.
[30] L. Zhao, et al., The role of sterilization in the cytocompatibility of titania nanotubes, Biomaterials 31 (8) (2010) 2055–2063.
[31] J. Park, et al., TiO_2 nanotube surfaces: 15 nm—an optimal length scale of surface topography for cell adhesion and differentiation, Small 5 (6) (2009) 666–671.
[32] J.H. Park, et al., Effect of cleaning and sterilization on titanium implant surface properties and cellular response, Acta Biomater. 8 (5) (2012) 1966–1975.
[33] M. Kulkarni, et al., Wettability studies of topologically distinct titanium surfaces, Colloids Surf. B: Biointerfaces 129 (2015) 47–53.
[34] M. Kulkarni, et al., Binding of plasma proteins to titanium dioxide nanotubes with different diameters, Int. J. Nanomedicine 10 (2015) 1359–1373.
[35] I. Junkar, et al., The role of crystallinity on polymer interaction with oxygen plasma, Plasma Process. Polym. 6 (10) (2009) 667–675.
[36] C. Canal, et al., Density of O-atoms in an afterglow reactor during treatment of wool, Plasma Chem. Plasma Process. 27 (4) (2007) 404–413.
[37] T. Mosmann, Rapid colorimetric assay for cellular growth and survival: application to proliferation and cytotoxicity assays, J. Immunol. Methods 65 (1) (1983) 55–63.
[38] Y. Liao, et al., A facile method to crystallize amorphous anodized TiO_2 nanotubes at low temperature, ACS Appl. Mater. Interfaces 3 (7) (Jul 2011) 2800–2804.
[39] A. Lamberti, et al., Ultrafast room-temperature crystallization of TiO_2 nanotubes exploiting water-vapor treatment, Sci. Rep. (2015) (5: p).
[40] O.K. Varghese, et al., Crystallization and high-temperature structural stability of titanium oxide nanotube arrays, J. Mater. Res. 18 (1) (2003) 156–165.
[41] D. Wang, et al., Spontaneous phase and morphology transformations of anodized titania nanotubes induced by water at room temperature, Nano Lett. 11 (9) (2011) 3649–3655.
[42] J. Yu, et al., Effect of crystallization methods on morphology and photocatalytic activity of anodized TiO_2 nanotube array films, J. Phys. Chem. C 114 (45) (2010) 19378–19385.
[43] R. Wang, et al., Photogeneration of highly amphiphilic TiO_2 surfaces, Adv. Mater. 10 (2) (1998) 135–138.
[44] W. Att, et al., The effect of UV-photofunctionalization on the time-related bioactivity of titanium and chromium–cobalt alloys, Biomaterials 30 (26) (2009) 4268–4276.
[45] T. Ueno, et al., Enhancement of bone–titanium integration profile with UV-photofunctionalized titanium in a gap healing model, Biomaterials 31 (7) (2010) 1546–1557.
[46] C. Wen, Surface Coating and Modification of Metallic Biomaterials, Woodhead Publishing, 2015.
[47] Y. Wang, et al., Biocompatibility of TiO_2 nanotubes with different topographies, J. Biomed. Mater. Res. A 102 (3) (2014) 743–751.